Elementary Excitations in the Cyclic Molecular Nanomagnet Cr_8

O. Waldmann,[1,*] T. Guidi,[2] S. Carretta,[3] C. Mondelli,[4] and A. L. Dearden[5]

[1]*Department of Physics, The Ohio State University, Columbus, Ohio 43210, USA*
[2]*Istituto Nazionale per la Fisica della Materia, Università Politecnica delle Marche, I-60131 Ancona, Italy*
[3]*Istituto Nazionale per la Fisica della Materia, Dipartimento di Fisica, Università di Parma, I-43100 Parma, Italy*
[4]*Istituto Nazionale per la Fisica della Materia, Institut Laue-Langevin, F-38042 Grenoble, France*
[5]*Department of Chemistry, University of Manchester, Manchester M13 9PL, United Kingdom*

(Received 2 May 2003; published 4 December 2003)

Combining recent and new inelastic neutron scattering data for the molecular cyclic cluster Cr_8 produces a deep understanding of the low lying excitations in bipartite antiferromagnetic Heisenberg rings. The existence of the L band, the lowest rotational band, and the E band, essentially spin wave excitations, is confirmed spectroscopically. The different significance of these excitations and their physical nature is clearly established by high-energy and Q-dependence data.

DOI: 10.1103/PhysRevLett.91.237202 PACS numbers: 75.50.Xx, 33.15.Kr, 75.75.+a, 78.70.Nx

Recent advances in inorganic chemistry resulted in compounds with some tens of magnetic metal ions linked by organic ligands forming well-defined magnetic nanoclusters. Being neither simple paramagnets nor bulk magnets, these molecular nanomagnets often exhibit fascinating quantum effects. For instance, quantum tunneling of the magnetization has been observed in the metal complexes Mn_{12} and Fe_8 [1].

Antiferromagnetic (AF) cyclic clusters represent another class of molecular nanomagnets. In these compounds the metal ions within a single molecule form almost perfect rings. The decanuclear wheel Fe_{10} has become the prototype [2], but wheels with different metal ions and varying (even) numbers of centers were realized [3]. The magnetization exhibits steplike field dependencies at low temperatures—a spectacular manifestation of quantum size effects in these nanomagnets [4].

Numerous experiments showed that these compounds are well described by the minimal spin Hamiltonian

$$H = -J\sum_{i=1}^{N}\mathbf{S}_i\cdot\mathbf{S}_{i+1} + D\sum_{i=1}^{N}S_{i,z}^2 + g\mu_B\mathbf{S}\cdot\mathbf{B}, \quad (1)$$

with isotropic Heisenberg coupling and weak uniaxial magnetic anisotropy of the easy-axis type (N is the number of spin centers, S_i the spin length with $\mathbf{S}_{N+1} = \mathbf{S}_1$, and z the uniaxial anisotropy axis) [5]. The Heisenberg interaction is dominant ($|D/J| < 0.03$); these objects are thus excellent experimental realizations of (bipartite) AF Heisenberg rings with weak magnetic anisotropy.

The observed steps in the magnetization curves provided a first phenomenological insight into the structure of the excitations of finite AF Heisenberg rings [2]. The lowest states are those with minimal energy for each value of the total spin $S = 0, 1, 2, \ldots$. Their energies follow the Landé rule $E(S) \propto S(S+1)$ as for a rigid rotator, and the notion of rotational modes was introduced [6]. A subsequent numerical study [7] showed that a complete description of the lowest lying excitations implies a set of $N-1$ parallel rotational bands [Fig. 1(b)]. These bands were divided into L and E bands according to the selection rule that all transitions from the L band to states neither belonging to the L nor to the E band (the quasicontinuum) have negligible transition matrix elements. The L and E bands reflect the fact that the Hamiltonian can be approximated by an interaction between the two sublattice spin vectors. The L band then corresponds to maximal sublattice spins, while the E band appears with one sublattice spin decreased by one [7,8]. For the states of the L band the shift quantum number q [9] toggles between $q = 0$ and $q = N/2$ as function of S; the E band embraces the lowest states with $q \neq 0, N/2$.

Recently, the cyclic cluster $[Cr_8F_8(L-d_9)_{16}]\cdot 0.25C_6H_{14}$ with $L = O_2CC(CH_3)_3$, or Cr_8, was investigated by inelastic neutron scattering (INS) [10]. The eight Cr^{3+} ions form an octagon linked by F ions and pivalate ligands. The experimental data were successfully fitted to Eq. (1) with $J = -1.46$ meV and $D = -0.038$ meV [5]. According to the numerical character of this analysis, however, no insight concerning the elementary excitations was obtained. In this work, these INS data are reanalyzed unearthing, in particular, the first experimental evidence for the E band. By adding new data clearly showing the different character of the L and E excitations and their physical nature, this work arrives at a complete experimental confirmation of the theoretical picture of the excitations in bipartite AF Heisenberg rings.

So far, basically all molecular nanomagnets of interest (including Mn_{12} and Fe_8 mentioned above) represent Heisenberg systems with weak anisotropy. It is thus of general importance to arrive at an understanding of the internal spin structure due to Heisenberg interactions. Remarkably, the L band was also found in other finite AF Heisenberg systems with completely different topology, theoretically [6,7] and experimentally [11]. Thus, the features which are confirmed here experimentally in

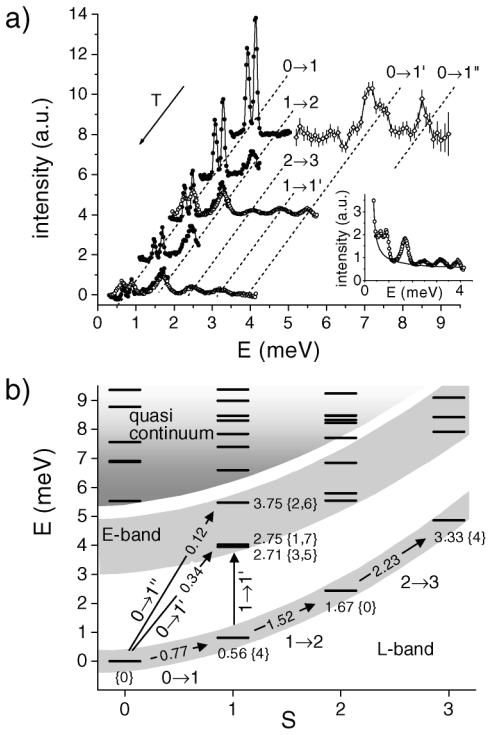

FIG. 1. (a) INS intensity versus energy transfer at different temperatures for Cr_8. Data recorded on IN6 with incident energy 2.35 meV at 2, 6, 12, 18, and 23 K (from back to front) are plotted as full circles, those with incident energy 4.86 meV at 12 and 21 K as open circles. Error bars are smaller than symbols. Open squares represent the MARI data at 2.5 K. For each curve, the background from the elastic peak and quasielastic contributions was fitted and subtracted from the data as shown in the inset for the IN6, 4.86 meV, 12 K data. The MARI data are enhanced by a factor of ≈ 10 with respect to the IN6 data. (b) Energy spectrum of an octanuclear spin-3/2 Heisenberg ring versus total spin quantum number S ($J = -1.46$ meV). Arrows indicate observed transitions and their labeling. Values at states give exact energies in units of $|J|$ and q in brackets. Values at arrows give the oscillator strengths $\langle n|S_i^z|m\rangle^2$. Zero-field splitting of spin multiplets due to magnetic anisotropy is omitted.

detail for AF Heisenberg rings are expected to be generic for a much broader class of AF Heisenberg systems [7].

Experiments were performed on 4 g of perdeuterated polycrystalline sample of Cr_8, prepared as described in [12]. High-energy-resolution INS experiments were done on the IN6 spectrometer of the Institute Laue-Langevin (Grenoble, France) with incident neutron energies of 2.35 and 4.86 meV for temperatures from 2 to 23 K. Measurements with energy transfer up to 15 meV were performed on the MARI spectrometer of the Rutherford Appleton Laboratory ISIS (Oxfordshire, United Kingdom) at a temperature of 2.5 K. The details of the experiments and data correction were as in [10].

The measurements of the INS intensity as functions of energy transfer are compiled in Fig. 1(a). The similarity of this figure with Fig. 3(c) in Ref. [7] is striking [13]. In Fig. 1(a) the $0 \rightarrow 1$ transition is split into two close peaks at 0.68 and 0.87 meV because of the magnetic anisotropy. The other transitions appear as single peaks because of their larger widths. The splitting of the $S = 1$ spin multiplet (0.19 meV) is smaller than its center of gravity (0.81 meV), showing that Cr_8 indeed represents an AF Heisenberg system with weak anisotropy. In the following, only averaged energies and integrated intensities will be discussed. The energy diagram for an octanuclear spin-3/2 Heisenberg ring is given in Fig. 1(b) with observed transitions indicated.

Apparently, the transitions $0 \rightarrow 1$, $1 \rightarrow 2$, and $2 \rightarrow 3$ correspond to transitions within the L band, the transitions $0 \rightarrow 1'$, $0 \rightarrow 1''$, and $1 \rightarrow 1'$ to transitions from the L band to the E band [7,13]. Thus, Fig. 1 establishes the first spectroscopic evidence for the L band and the first experimental evidence for the E band. The characteristic properties of the two types of bands will be explored in more detail in the following. The transition energies for the $1 \rightarrow 1'$ and the L-band transition $3 \rightarrow 4$ are very close in Cr_8. The peak assigned as $1 \rightarrow 1'$ in Fig. 1(a) thus actually consists of two distinct contributions and will not be considered further.

The experimentally determined and theoretically expected energies and transition matrix elements are listed in Table I. As thermal population has to be accounted for in the determination of the matrix elements, the given errors for the matrix elements also reflect the good agreement of observed and expected temperature dependence of peak intensities. With $J = -1.46$ meV [10] the agreement between experimental and exact energies of an octanuclear spin-3/2 Heisenberg ring [Fig. 1(b)] is excellent. Table I also demonstrates that the energies of the L-band states closely follow the Landé rule. As a further characteristic of the L band, the oscillator strengths (which are proportional to the $|M|^2$ of Table I) for the $S \rightarrow S + 1$ transitions increase as $f_S = f_0(S + 1)$ [7]. In view

TABLE I. Energies of the spin multiplets as determined from experiment, from exact calculations [see Fig. 1(b)] using $J = -1.46$ meV [10], and from the Landé rule $E(S) = \Delta/2S(S + 1)$ with $\Delta = E(1) - E(0)$. Also given are experimental intensities $|M|^2$ corrected for thermal population, different Q ranges, and k_f/k_i ratios. The intensity for the $0 \rightarrow 1''$ transition was obtained by calibrating the MARI data against the IN6 data by matching the matrix elements for the $0 \rightarrow 1'$ transition.

Multiplet	Energy (meV)	Exact (meV)	Landé (meV)	Transition	$\lvert M\rvert^2$ (a.u.)
$S = 1$	0.80(1)	0.816	0.816	$0 \rightarrow 1$	0.78(6)
$S = 2$	2.46(3)	2.44	2.45	$1 \rightarrow 2$	2.2(2)
$S = 3$	4.94(3)	4.87	4.90	$2 \rightarrow 3$	3.7(2)
$S = 1'$	3.82(7)	3.99	⋯	$0 \rightarrow 1'$	0.38(4)
$S = 1''$	5.24(5)	5.48	⋯	$0 \rightarrow 1''$	0.23(7)

of the experimental difficulties to determine $|M|^2$, this behavior is well observed in experiment.

The E band essentially represents AF spin wave excitations [7]. In the classical limit, these are expected at energies $\epsilon(q) = 2S_i|J \sin(q2\pi/N)|$ [14,15]. The four $S = 1'$ spin levels belong to $q = 1, 7$ and $q = 3, 5$, the $S = 1''$ spin levels to $q = 2, 6$ [Fig. 1(b)]. The spin wave nature of these states is indicated by the agreement of the observed energies with $\epsilon(q = 1, 3, 5, 7) = 3.10$ meV and $\epsilon(q = 2, 6) = 4.38$ meV, especially as these values should be larger for $S_i = 3/2$ by several 10% due to quantum effects [15,16]. The observed E-band transition intensities further confirm this picture: $|M|^2$ is (i) significantly smaller than for the L transitions and (ii) larger for $0 \rightarrow 1'$ than for $0 \rightarrow 1''$ reflecting the expected $\sqrt{1 - \cos(q2\pi/N)}/\sqrt{1 + \cos(q2\pi/N)}$ dependence [15].

A critical test of the internal structure of the wave functions is provided by the selection rule distinguishing L and E bands: The oscillator strengths for transitions from the L band to states of the quasicontinuum are virtually zero [7,15]. As they cannot be calibrated precisely, the experimental oscillator strengths do not allow us to show this directly from sum rules [7]. But Fig. 2, presenting an INS measurement for energies up to 13 meV, demonstrates that at low temperatures no further transitions than the $0 \rightarrow 1$, $0 \rightarrow 1'$, and $0 \rightarrow 1''$ transitions could be detected. If it were not for the selection rule, several transitions starting at 6.5 meV were to be expected; see Fig. 1(b). This provides the most compelling evidence that the wave functions of the states of the rotational bands are "classical" in nature [7] (hereafter, classical is used in the sense of Ref. [8]).

The different nature of the L and E excitations, in turn, becomes most apparent from the Q dependence of the INS intensity. Experimental results are shown in Fig. 3 for the L transitions $0 \rightarrow 1$, $1 \rightarrow 2$, $2 \rightarrow 3$, and the E transition $0 \rightarrow 1'$, respectively. For the L transitions, the Q dependencies are very similar to each other and exhibit a pronounced oscillatory behavior, in clear contrast to the almost flat Q dependence of the E transition.

Because of the high spatial symmetry of cyclic clusters, the Q dependence of the INS intensity can be calculated analytically [17]. Classifying eigenstates as $|\tau q\rangle$, τ denoting further quantum numbers, the Q dependence is, up to a constant factor, completely specified by the transfer in shift quantum number $\Delta q = q - q'$ (and the radius of the ring, 4.427 Å), for all transitions within the L band hold $\Delta q = N/2$. For transitions from the L to the E band one has to take into account the degeneracy of spin levels with q and $N - q$ as enforced by symmetry and quasidegeneracies due to the $|\sin(q2\pi/N)|$-like dependence of energy on q which cannot be resolved experimentally. Accordingly, the transition $0 \rightarrow 1'$ is the sum of four transitions with $\Delta q = 1$, 3, 5, and 7. The theoretical curves are also presented in Fig. 3. The agreement with experiment is convincing. This analysis provides a direct determination of the different spatial symmetry properties of the L and E bands and demonstrates a Néel structure of the L-band wave functions.

Figure 3(a) indicates that the intensity of the $0 \rightarrow 1$ transition does not drop to zero for $Q \rightarrow 0$, in contrast to the theoretical curve. This is also evident with better

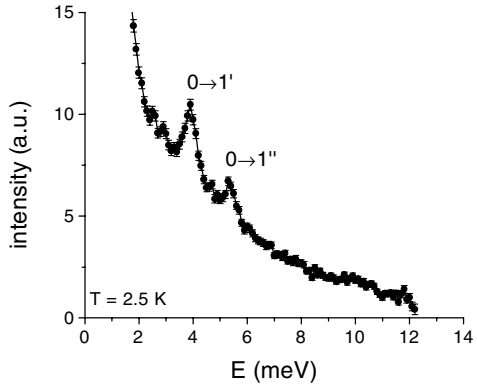

FIG. 2. INS intensity at 2.5 K recorded on MARI with 15 meV incident neutron energy, integrated over the momentum range $0 < Q < 1.5$ Å^{-1}. The observed peaks were assigned as indicated. At low energies, the quasielastic peak dominates.

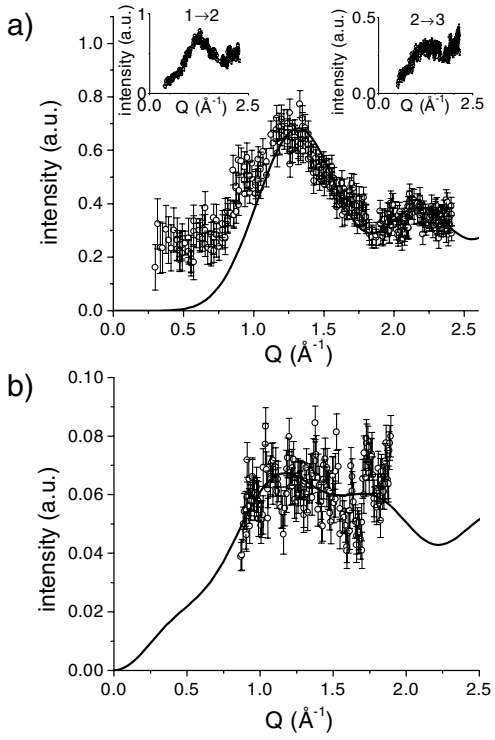

FIG. 3. Integrated intensity versus momentum transfer Q for (a) the $0 \rightarrow 1$ transition (insets: $1 \rightarrow 2$ and $2 \rightarrow 3$ transitions) and (b) the $0 \rightarrow 1'$ transition. Data were obtained on IN6 with 4.86 meV incident energy at 12 K. The solid lines represent the theoretical curves as calculated for (a) a transition with $q = 0 \rightarrow q' = 4$ and (b) the sum of transitions $q = 0 \rightarrow q' = 1$, 3, 5, and 7. Curves were scaled by a constant factor.

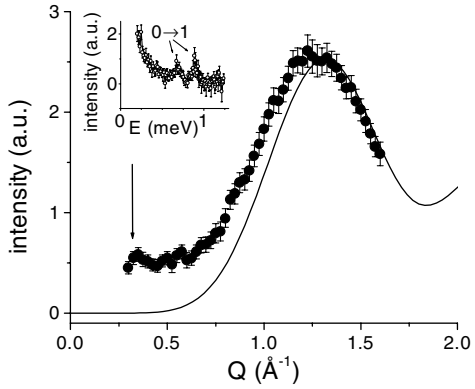

FIG. 4. Integrated intensity versus momentum transfer Q for the $0 \rightarrow 1$ transition as obtained on IN6 with 2.35 meV incident energy at 2 K. The solid line represents the theoretical curves as calculated for a transition with $q = 0 \rightarrow q' = 4$. The curve was scaled by a constant factor. The inset shows the intensity versus energy at 2 K. The peak at 0.7 meV corresponds to $Q = 0.317$ Å^{-1}, the peak at 0.9 meV to $Q = 0.344$ Å^{-1}.

resolution from the 2 K data shown in Fig. 4. The inset explicitly shows the presence of INS intensity at low Q. For cyclic clusters, because of their symmetry, the INS intensity drops to zero quadratically in Q for $q \neq q'$, i.e., follows $\delta_{q,q'} + \mathcal{O}(Q^2)$ for $Q \rightarrow 0$ [17]. Accordingly, the observed nonzero intensity for $Q \rightarrow 0$ suggests that the spin Hamiltonian for Cr_8 has to be extended by small terms with lower symmetry. Such terms are currently under strong debate [18,19] as they would represent sources of decoherence for a mesoscopic tunneling of the Néel vector, which was predicted for cyclic clusters [20]. INS at low momentum transfer can be a powerful tool to detect and analyze these terms.

The E band was identified as spin waves. In contrast, the above experiments unambiguously demonstrated the Néel-like structure of the L band: it exactly represents the degrees of freedom due to a combined rotation of the oppositely oriented total spins on each sublattice as they appear in the spin wave theory of antiferromagnets [14] (a nice description is given in [21]). Accordingly, in the limit of infinite N the L band would evolve into the essentially classical Néel ground state, if it were not for the strong quantum fluctuations in one-dimensional chains.

Thus, finite AF Heisenberg rings, approximated experimentally by molecular cyclic clusters, are rather classical and in this sense closer to higher dimensional than to one-dimensional AF systems. The internal spin structure of cyclic clusters, as confirmed here by experiment, is well described by the usual spin wave theory for antiferromagnets. The important new feature in these systems, however, is that the lowest excitations as relevant for low temperature experiments are not the spin wave excitations as in extended antiferromagnets, but the quantized rotation of the Néel-type ground state configuration.

By extension, this suggests that for Heisenberg systems, where the correct ground state is obtained by a classical assignment of up and down spins to each center as it is the basis for the Néel state, a (semi)classical approach is adequate. This includes a large number of molecular systems, e.g., the cyclic metal clusters, the iron icosidodecahedron $\{Mo_{72}Fe_{30}\}$ [11], and molecular grids [22], but also single molecule magnets like Mn_{12} and Fe_8. We conclude: In the majority of cases the internal spin structure of molecular nanomagnets, being truly quantum mechanical objects, is essentially classical.

We thank R. Caciuffo, G. Amoretti, and V. Dobrovitski for enlightening discussions and C. D. Frost for help with INS experiments. We thank the Deutsche Forschungsgemeinschaft, the Department of Energy (Grant No. DE-FG02-86ER45271), and the FIRB program of the Italian Ministry of University and Research.

*Email address: waldmann@mps.ohio-state.edu

[1] A. Caneschi *et al.*, J. Magn. Magn. Mater. **200**, 182 (1999).
[2] K. L. Taft *et al.*, J. Am. Chem. Soc. **116**, 823 (1994).
[3] R.W. Saalfrank *et al.*, Angew. Chem., Int. Ed. **36**, 2482 (1997); A. L. Dearden *et al.*, *ibid.* **40**, 151 (2001).
[4] D. Gatteschi *et al.*, Science **265**, 1054 (1994).
[5] A dipole-dipole interaction is not negligible, but has similar effects as the single-ion terms $S_{i,z}^2$. The D value should be understood as to include both contributions.
[6] J. Schnack and M. Luban, Phys. Rev. B **63**, 014418 (2000).
[7] O. Waldmann, Phys. Rev. B **65**, 024424 (2001).
[8] A. Honecker *et al.*, Eur. Phys. J. B **27**, 487 (2002).
[9] The cyclic symmetry implies a shift quantum number q defined here via the shift operator $\mathbf{T}|q\rangle = e^{iq2\pi/N}|q\rangle$.
[10] S. Carretta *et al.*, Phys. Rev. B **67**, 094405 (2003).
[11] J. Schnack, M. Luban, and R. Modler, Europhys. Lett. **56**, 863 (2001).
[12] J. van Slageren *et al.*, Chem. Eur. J. **8**, 277 (2002).
[13] In Ref. [7], the transitions $0 \rightarrow 1$, $1 \rightarrow 2$, $2 \rightarrow 3$ were denoted as L^1, L^2, L^3, the transitions $0 \rightarrow 1'$, $0 \rightarrow 1''$, $1 \rightarrow 1'$ as E_1^{0+}, E_2^{0+}, E_1^1, respectively.
[14] P.W. Anderson, Phys. Rev. **86**, 694 (1952).
[15] G. Müller, Phys. Rev. **26**, 1311 (1982).
[16] S. Itoh *et al.*, Phys. Rev. Lett. **74**, 2375 (1995).
[17] O. Waldmann, Phys. Rev. B **68**, 174406 (2003).
[18] M. Affronte *et al.*, Phys. Rev. Lett. **88**, 167201 (2002).
[19] O. Waldmann *et al.*, Phys. Rev. Lett. **89**, 246401 (2002).
[20] A. Chiolero and D. Loss, Phys. Rev. Lett. **80**, 169 (1998).
[21] P.W. Anderson, *Basic Notions of Condensed Matter Physics* (Benjamin/Cummings Publishing Co., Menlo Park, 1984), p. 44.
[22] O. Waldmann *et al.*, Phys. Rev. Lett. **88**, 066401 (2002).